LAGRANGIAN NAVIER-STOKES FLOWS: A STOCHASTIC MODEL

MARC ARNAUDON, ANA BELA CRUZEIRO, AND NUNO GALAMBA

Abstract. We associate stochastic Lagrangian flows to Navier-Stokes (deterministic) velocities and show their unstable behaviour.

Contents

1. Introduction

The Navier-Stokes system

$$\frac{\partial}{\partial t}u = -(u.\nabla)u + \nu\Delta u - \nabla p,\ div\ u = 0 \tag{1.1}$$

models the time evolution of the velocity field of incompressible fluids with viscosity $\nu \geq 0$.

The Lagrangian approach to hydrodynamics studies the configuration of the underlying particles, namely the solutions of the equations

$$\frac{d}{dt}g(t) = u(t, g(t))$$

whereas the Eulerian approach deals with the time evolution of the velocities. We stress the fact that there is no simple relation between the Eulerian and Lagrangian description of the fluid motion (c.f., for instance, [1] or [6]).

Turbulent regimes are often studied in the perspective of the theory of dynamical systems as chaotic systems, which are characterized by a strong sensitivity to initial conditions. For example reference [6] follows this point of view, mainly using Lyapounov exponents to describe the stability properties of the dynamical system trajectories. The fact that a simple regular Euler flow can give rise to chaotic particle trajectories, a phenomenon which has been intensively studied by the Dynamical Systems community, is also present in Fluid Dynamics. For example two dimensional chaotic behaviour in Stokes flows was considered in various works, starting with [1].

In the case of vanishing viscosity V. I. Arnold ([3]) described the Lagrangian configuration as a geodesic flow on a space of diffeomorphisms (regular bijections of

the underlying space where the particles move) preserving the volume measure. As a geodesic the corresponding flow $g(t)$ satisfies a variational principle: it minimizes, in a time interval $[0, T]$, the action functional

$$S[g] = \frac{1}{2} \int_0^T \int |\frac{d}{dt} g(t)(x)|^2 dx \tag{1.2}$$

Based on the Lagrangian approach to hydrodynamics initiated by Arnold the instability of trajectories of the corresponding flows, that is, the exponential divergence of their distance, was derived (c.f. [4] and references therein).

In the dissipative case (non zero viscosity) one should expect Lagrangian trajectories to become closer and closer after some possible initial stretching. On the other hand a non-conservative system cannot admit a standard geodesic formulation. So the problem of establishing a variational principle for viscosity lagrangian flows and the study of their stability properties is a non trivial one.

Here we describe an alternative perspective on Lagrangian flows. To a (deterministic) velocity solving Navier-Stokes equations we associate random Lagrangian flows. These are stochastic processes whose mean velocity is precisely the deterministic Navier-Stokes field. The model is justified by the fact that these flows are solutions of a (now stochastic) variational principle that extends Arnold's one to the viscous case and reduces to it when $\nu = 0$. This approach was initiated in works such as [14], and more recently developed rigorously in [10] for flows living on the flat torus and in [2] for flows in a general compact Riemannian manifold.

We stress that this is, by no means, a stochastic perturbative approach. We do not add stochastic forces to the Navier-Stokes dynamics, we do not consider additional phenomena such as diffusivity. Also the randomness is not chosen *ad hoc*. It is hidden in Navier-Stokes equation itself, as quantum randomness is hidden in Schroedinger equation. The stochastic process we study is the one that minimizes the (mean) energy and its diffusive part is responsible for the second order term in the Navier-Stokes vector field which corresponds to the mean velocity field of this stochastic Lagrangian flow. In other words the Laplacian term in the Navier-Stokes equation for the velocity expresses already the whole randomness of the system. Furthermore, as the Laplacian is defined according to the geometry of the configuration space, the Brownian part of the Lagrangian stochastic flows is determined by this geometry. This approach is therefore an alternative description of the motion of particles.

The stability properties of the Lagrangian stochastic flows that we consider here as well as the evolution in time of the rotation between particles were studied in [2], with a particular emphasis for the torus case. There it was shown that instability was to be expected, depending on the geometry of the underlying configuration space. The behaviour of some particular flows is considered in this work. We show that the distance between random Lagrangian particles increases with time significantly more than the distance of their deterministic counterpart.

Even when the corresponding deterministic description is not chaotic, the stochastic picture may, as shown in our examples, have initially nearby trajectories diverging faster than exponentially.

The nondeterministic and chaotic behaviour of Lagrangian trajectories, at least at high Reynolds numbers but also in the case of some laminar flows has been pointed out for a long time (c.f. for example [7] and references therein). Partly the phenomena has been connected to the nonregularity of velocity fiels, lack of

uniqueness of the solution, etc, and this leads to the study of "generalized flows", where various types of regularization of the velocity fields are considered (c.f. [8]). In the paper [5] the authors studied a model where the velocity is a Gaussian random field and they connected the stochasticity of the motion with sensitive dependence on initial conditions.

In our model the (mean) velocities are deterministic functions, coinciding precisely with smooth solutions of the Navier-Stokes equation. The model is, in this sense, similar to the one in [9]. It provides stochastic Lagrangian trajectories for all values of the viscosity. It involves, in contrast with other approaches, a choice of randomness which is not canonical and may depend on various parameters. In particular this randomness may have its origin in excited small or large modes (large or small lenght scales). It is also much linked to the geometry of the underlying configuration space. The possible mathematical versions of the model may not all correspond to physical relevant ones.

Diffusions driven by various (even infinitely many) independent Brownian motions were also considered in [13]. They were studied in depth concerning separation of particle flows, their coalescence and hitting properties, along the evolution. Nevertheless in this work special attention is given to the case where the covariance of the motion is non smooth, which is not the case treated here.

The exponential type separation of particles is, in a counter-intuitive way, enhanced by the viscosity parameter in cases where the stochastic component of the motion is very strong when compared with the deterministic one. This may indicate that the choice of noise and its parameters should be carefully made on a physical basis, since the behaviour is model dependent.

Stochastic Lagrangian paths also appear in representation formulae for the Navier-Stokes solutions, as in [11]. Those perspectives are quite distinct from ours.

We mention a different view on Lagrangian trajectories for the Navier-Stokes equation as geodesics for some geometry which is constructed in [15]. There the approach is deterministic: what is deformed to pass from Euler to Navier-Stokes is the geometry. In contrast, in our case, the deformation is stochastic.

2. The stochastic Lagrangian picture

On the two-dimensional torus $\mathbb{T} = \mathbb{R}/2\pi\mathbb{Z} \times \mathbb{R}/2\pi\mathbb{Z}$ we consider the following vector fields, for $k = (k_1, k_2) \in \mathbb{Z}^2$,

$$A_k(\theta) = k^\perp \cos k.\theta, \quad B_k(\theta) = k^\perp \sin k.\theta$$

where $k^\perp = (k_2, -k_1)$. A divergence free square integrable vector field v with real components on the torus can be represented by its Fourier expansion as $u(\theta) = \sum_k (u_k^1 A_k(\theta) + u_k^2 B_k(\theta))$.

Consider the stochastic process $W(t)$ defined by

$$dW^{\tilde\nu}(t)(\theta) = \sum_{k\in\mathbb{Z}} \lambda_k \sqrt{\tilde\nu} \left(A_k(\theta) dW_k(t) + B_k(\theta) d\tilde W_k(t) \right) \tag{2.3}$$

with fixed initial condition $W(0)$, where $W_k, \tilde W_k$ are independent copies of real Brownian motions and the derivative d means Itô derivative in time, $\tilde\nu \geq 0$. We assume that $\sum_k |k|^2 \lambda_k^2 < \infty$, where $|k|^2 = k_1^2 + k_2^2$, which is a necessary and sufficient condition for the stochastic process to be well defined and square integrable as a

function of the space variable θ. In fact, in the examples presented in the next section we consider only a finite number of such λ_k (only a finite number of Fourier modes will be considered random). Furthermore we assume $\lambda_k = \lambda(|k|)$ to be nonzero for an equal number of k_1 and k_2 components. For a time-dependent vector field $u(t,\theta)$, let g_u denote the solution of the following stochastic differential equation

$$dg_u(t) = dW^{\tilde{\nu}}(t) + u(t, g_u(t))dt \tag{2.4}$$

with initial condition $g_u(0)(\theta) = \theta$. Then the generator of the process for functions on the torus is equal to

$$L_u = c\tilde{\nu}\Delta + \frac{\partial}{\partial t} + \partial_u$$

with $2c = \sum_k \lambda_k^2$ (c.f. [10]). Namely, for a smooth function f defined on the torus, if $\eta_t(\theta) = Ef(g_u(t)(\theta))$, we have

$$\frac{\partial}{\partial t}\eta_t = L_u\eta_t$$

Notice that when $\tilde{\nu} = 0$ the last relation is just the total derivative of f along the corresponding (deterministic) flow $g_u(t)$. It is the presence of the Laplacian term, the generator of the Brownian part of the process, which will be responsible for the Laplacian term in Navier-Stokes equation.

We remark that other Brownian processes can give rise to the same generator. In other words, the choice of randomness in the model is not unique.

We define the mean derivative of $g_u(t)$ as its drift or, more precisely, if E_t denotes the conditional expectation with respect to the past of t filtration,

$$D_t g_u(t) = lim_{\epsilon\to 0}\frac{1}{\epsilon}(E_t(g_u(t+\epsilon) - g_u(t))$$

then

$$D_t g_u(t) = u(t, g_u(t))$$

This notion generalizes for non differentiable trajectories the usual time derivative: when the viscosity is zero the process $g_u(t)$ is the Lagrangian (deterministic) flow for the Euler equation.

We claim that, when the vector field u satisfies Navier-Stokes equations, the process g_u gives a Lagrangian description of the motion. In fact one can define a stochastic action functional as

$$S[g] = \frac{1}{2}\int_0^T \left(\int_{\mathbb{T}} |D_t g_u(t)(\theta)|^2\, d\theta\right) dt \tag{2.5}$$

where $d\theta$ stands for the normalized volume measure on the torus.

Then (c.f.[10] and [2] for more details and proofs), a process g_u of the form (2.4) is critical for the action functional (2.3) if and only if the drift u satisfies Navier-Stokes equations (1.1) with viscosity coefficient $\nu = \frac{\tilde{\nu}}{2}\sum_k \lambda_k^2$.

Again we notice that when the viscosity is zero the action reduces to (1.1) and we obtain the variational principle for the Euler equation.

In this work we shall only consider the case where the configuration space is the two-dimensional torus or the whole plane. Following the construction in [6], one can work in a general compact Riemannian manifold the Laplacian and therefore

the associated Brownian motion will be defined by the corresponding Riemannian metric.

3. Stability of motion and rotation of particles; examples

Take two different solutions of the stochastic differential equation (2.4), $g_u(t)$ and $\tilde{g}_u(t)$, starting respectively from $g_u(0)(\theta) = \phi(\theta)$ and $\tilde{g}_u(0)(\theta) = \psi(\theta)$, with $\phi \neq \psi$ Then we can use Itô formula to explicitely compute the evolution in time distance between the two solutions. By considering the L^2 distance, namely

$$d^2_{L^2}(g_u(t), \tilde{g}_u(t)) = \int |g_u(t)(\theta) - \tilde{g}_u(t)(\theta))|^2 d\theta$$

we have shown in [2] that, at least until some time which depends on $\|\phi - \psi\|_\infty$ and also on the initial velocity $u(0, .)$, the L^2 distance between the Lagrangian flows increases more than exponentially.

Here we numerically analyse the behaviour of the distance between Lagrangian stochastic particles in two examples, one in the torus and the other in the plane. The distance we refer to here is the standard ponctual distance between trajectories. We observe that they are, indeed, more unstable then the classical deterministic ones, and this is specially the case after some initial short time when the deterministic trajectories get apart.

Also in [2] we have studied the behaviour of the unit tangent vector to the curve linking $g_t(\theta)$ and $\tilde{g}_t(\theta)$ and its evolution in time. In the case of the two dimensional torus it was deduced that the rotation between particles for short distances between particles becomes more and more irregular the shorter the distance. The effect is stronger for bigger values of the quantity $\nu \sum_k \lambda_k^2 |k|^4$. We observe this phenomenon in our example of the torus.

Example 1. A stochastic flow on the two-dimensional torus.

We consider the following time-dependent vector field on the torus $\mathbb{T}$

$$u(t, \theta) = c_1 \sum_{k \in K} k^\perp e^{-\nu |k|^2 t} \cos(k.\theta) + c_2 \sum_{k \in K} k^\perp e^{\nu |k|^2 t} \sin(k.\theta)$$

The sums are over some set of indexes $K \subset \mathbb{Z}^2$ and $k.\theta = k_1\theta_1 + k_2\theta_2$. For every c_1, c_2 the vector field u is a solution of Navier-Stokes equation with zero gradient of pressure. Let g_u be the corresponding Lagrangian flow solving the stochastic differential equation,

$$dg_u(t) = \sum_k \lambda_k \sqrt{\tilde{\nu}}(k_2, -k_1) \cos(k.g_u(t)) dW_k(t)$$

$$+ \sum_k \lambda_k \sqrt{\tilde{\nu}}(k_2, -k_1) \sin(k.g_u(t)) d\tilde{W}_k(t) + u(t, g_u(t)) dt \tag{3.6}$$

with ν and $\tilde{\nu}$, as before, related as $\tilde{\nu} = \frac{\nu}{2} \sum_k \lambda_k^2$.

The differential equations were numerically solved, through the Monte Carlo method, with the Euler-Maruyama algorithm (c.f., for example, [12]) with a time-step $\delta t = 2^{-10}$. Emphasis was placed on the behavior of the trajectories at short

times and different sets of parameters were considered to probe the differences between the deterministic and stochastic trajectories. Unless stated otherwise, in the respective plots, the following parameters were used in the calculations: the sums over k in (3.6) were carried out for 6 vectors, $k_1 = (0,1), k_2 = (1,0), k_3 = (1,1)$ and $k_i^{\perp}, i = 1,2,3$. This set of indexes is denoted hereafter by K^a and it was used in the sums over k for the stochastic and deterministic components, although other values were also considered for the latter. We have considered $c_1 = c_2 = 1.5$, the kinematic viscosity $\nu = 1.0$ and $\lambda_k = 0.7$ for k = 1,2,3, $\lambda_{k^\perp} = \lambda_k$. The c_j, with $j = 1,2$ and the λ_k with $k = 1,2,3$, were kept equal for every j and k, respectively, for simplicity's sake. We shall refer to the solutions of the stochastic differential equation (3.6), simply as stochastic trajectories, in opposition to the deterministic trajectories (i.e., the Navier-Stokes solution trajectories).

Figure 1 displays the effect of different parameters on a single deterministic trajectory starting at the point $(0.0, 0.0)$. The differential equation was solved over $[0,T]$, with $T = 50$. This value is large enough to plot the complete deterministic trajectories for the different parameters considered. As it may be seen the trajectory length increases with the value of $c_1 (= c_2)$, whereas it decreases with the increase of both, the kinematic viscosity, ν, and the magnitude of the components of the k vectors.

A comparison between some of the deterministic trajectories depicted in Fig. 1 and the corresponding stochastic trajectories is shown in Fig. 2. The latter are averages over 50 Brownians. The equations were solved within the interval $[0,T]$, with $T = 4$, plot (a), $T = 5$, plot (b), and $T = 1$, plot (c). Notice that the deterministic trajectories in Fig. 2, plots (a), (b) and (c), are the dashed (red) lines plotted respectively in Fig. 1, (a), (b) and (c). The plots (a) and (b) of Fig. 2 allow comparing the effect of ν, whereas the plots (a) and (c) allow comparing the effect of the k vectors on the trajectories.

Concerning the rotations between particles, the stochatic component of the motion induces an opposite behaviour regarding the effect of ν and the magnitude of the components of the k vectors. Thus, the space spanned by the stochastic trajectory increases with ν as well as with the magnitude of the components of the k vectors.

Figure 3 depicts two deterministic trajectories and their stochastic counterparts. Their ponctual distance (the expected values of the distance for the later) are also plotted. The trajectories start at the points $(0.0, 0.0)$ and $(0.01, 0.01)$, and were computed using the same parameters of Fig. 2, plots (a) and (b). The equations were solved within $[0,T]$, with $T = 1$. The stochastic trajectories and the respective expected values of the distance are averages over 25000 Brownians. Examination of the plots (a2) and (b2) of Fig. 3 shows that the expected values of the distance between the stochastic trajectories increase significantly faster than their deterministic equivalent. Specifically, the expected values of the distance between the stochastic trajectories depict an approximately exponential growth at short times ($t < 1$). Moreover it can be seen that the distance between the random trajectories increases faster for larger kinematic viscosities (compare the red dashed lines in (a2) and (b2)). This trend is opposite to that depicted by the deterministic trajectories and it reflects a larger microscopic uncertainty on the particles' positions, resulting from the stochastic term being multiplied by the

square root of $\tilde{\nu}$, proportional to ν. This behavior, however, as we shall see, is also parameter dependent, and more importantly, it depends on $u(t,\theta)$, through θ.

A comparison between the deterministic and respective stochastic trajectories within $[0,T]$, with $T=5$ is shown in Figs. 4 and 5 for two distinct sets of deterministic k vectors, K^a and K^b, and different values of ν. The choice K^b correspond to bigger Fourier modes (or smaller lenght scales). The stochastic component was kept unchanged, i.e., both sets of solutions were obtained for K^a. The distance between the deterministic trajectories and the expected distance for the stochastic trajectories is also displayed. The stochastic solutions for both, K^a and K^b, depict an inward trajectory in opposition with the outward rotations of the deterministic trajectories. Further it is possible to observe an inversion, for K^a, (Fig. 4 (a2) and (b2)), of the dependence on the viscosity in passing from the deterministic to the stochastic trajectories. This is the situation described previously regarding the results plotted in Fig. 3. However, for K^b the observed trend is similar for both, the deterministic and stochastic trajectories. This behavior, depicted in Fig. 5 (b2), for the expected values of the distance between the stochastic trajectories is observed only at short times. Thus, at larger times the trend observed in Fig. 4 (b2) will be recovered as the drift approaches zero. Further, we can see, that the stochastic Lagrangian flow leads to more unstable trajectories when compared with the deterministic case, for both K^a and K^b.

We now turn attention to the influence of the velocity field, through its explicit dependence on θ, on the stochastic trajectories. For this purpose we considered trajectories starting at different points in the torus. Here we present results for the viscosity dependence on the expected distance between two trajectories starting at points (1.0,1.0) and (1.01,1.01). The velocity field driving these trajectories is significantly different from that for the points (0.0,0.0) and (0.01,0.01) previously described. These results have been obtained using the same parameters as in Fig. 4 and are displayed in Figure 6. As it may be seen, the behavior with viscosity is similar for both the stochastic and deterministic trajectories, in opposition with the results found for the trajectories starting at (0.0,0.0) and (0.01,0.01). The reason is that the drift is significantly stronger than that in Fig. 4. Notice that the deterministic trajectories (see Fig. 6 (a2)) also diverge much faster than those depicted in Fig. 4 (a2). This is similar to the situation in Fig. 5 where the deterministic trajectories also diverge faster for K^b than for K^a.

The examples presented here for the torus show, therefore, that the stochastic trajectories diverge significantly faster than their deterministic equivalent, following our expectations. In the following section we provide a different example for a distinct solution of the Navier-Stokes equation in 2-dimensions.

Example 2. The Taylor-Green vortex solution.

Let us now consider the Taylor-Green vortex solution of the Navier-Stokes equation on the plane with viscosity ν,

$$v(t,x,y) = (\sin x \cos y, -\cos x sin y) e^{-2\nu t}$$

Here the pressure is equal to $p(t,x,y) = \frac{1}{4}(\cos^2 x + \cos^2 y) e^{-4\nu t}$.

Consider the corresponding stochastic Lagrangian trajectories,

$$dg_v(t) = \sum_k \lambda_k \sqrt{\tilde{\nu}} k^{\perp} \cos(k.g_v(t)) dW_k(t)$$

$$+ \sum_k \lambda_k \sqrt{\tilde{\nu}} k^{\perp} \sin(k.g_v(t)) d\tilde{W}_k(t) + v(t, g_v(t))dt \tag{3.7}$$

The trajectories were computed using a similar approach to the one described previously for Example 1. Parameters λ_k are kept equal, $\lambda_k = 0.5$ and $\lambda_k^{\perp} = \lambda_k$, for $k = 1, 2, 3$ and we use the set of k vectors of Example 1, denoted by K^a, for the stochastic component. A similar time-step to that of Example 1 was used (i.e., $\delta t = 2^{-10}$).

Figure 7 shows the expected value of the distance between trajectories starting at $(1.0, 1.0)$ and $(1.01, 1.01)$ for two distinct viscosities. The equations were solved within $[0, T]$, with $T = 5$. As in Fig. 3 the stochastic trajectories and the respective expected values of the distance are averages over 25000 Brownians. A similar behavior to that depicted in Fig. 3 of Example 1 can be observed. Thus, $[E]$ increases significantly faster for the random trajectories than the distance between the deterministic trajectories.

4. Conclusions

We propose a description of the Lagrangian evolution associated to Navier-Stokes equations in terms of stochastic processes. These processes are solutions of stochastic differential equations whose diffusion coefficients generate the Laplacian term in the Navier-Stokes equations and whose drifts (or mean velocities) coincide with their smooth solutions. They satisfy a least action stochastic principle. So we propose to study non-smooth particle trajectories associated with smooth velocities.

We study the model behaviour concerning the separation of trajectories along the time, specially in the case of the torus. Since there are many Browninan motions giving rise to the same Laplacian, our stochastic processes do not follow a canonical choice and the corresponding behaviour depends on the geometry, on the lenght scales that are "excited" by noise and on the initial values of the position and velocity. Nevertheless we always obtain a larger separation for the stochastic trajectories as compared to the classical trajectories counterpart.

Figures

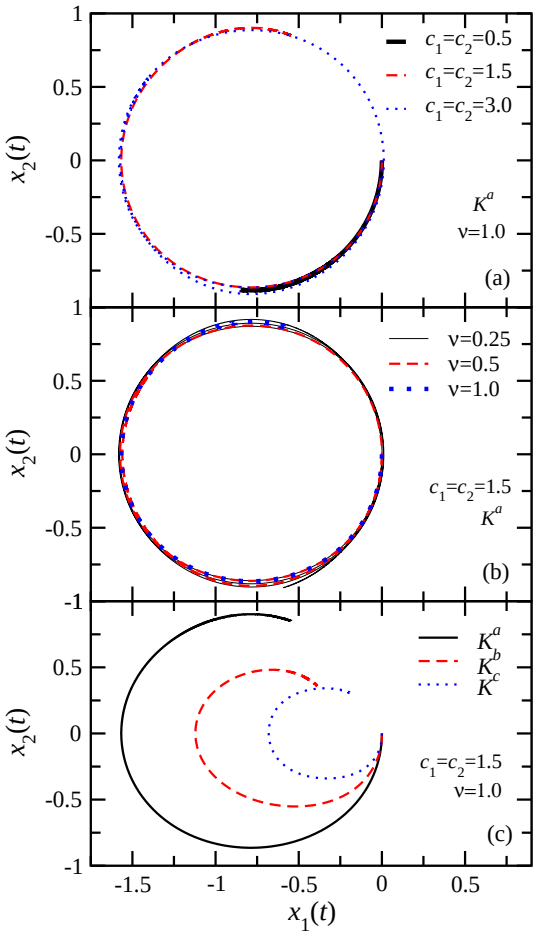

FIGURE 1. Deterministic trajectories for different (a) values of $c_1(=c_2)$, (b) kinematic viscosities, ν, and (c) deterministic k vectors, where K^a denotes the set $\{(0,1),(1,0),(1,1);k_i^{\perp},i=1,2,3\}$, K^b denotes $\{(1,1),(1,2),(2,1);k_i^{\perp}\}$ and K^c denotes $\{(2,2),(2,3),(3,2);k_i^{\perp}\}$.

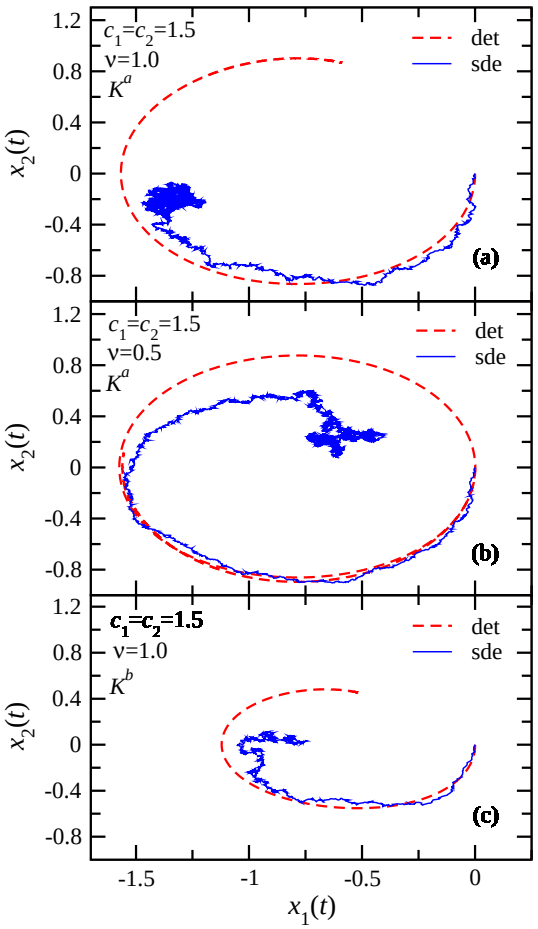

FIGURE 2. Comparison between deterministic and stochastic trajectories for different parameters; K^a and K^b are as in Fig. 1 for the deterministic sums over k. The sums over k for the stochastic part are for K^a in the three plots.

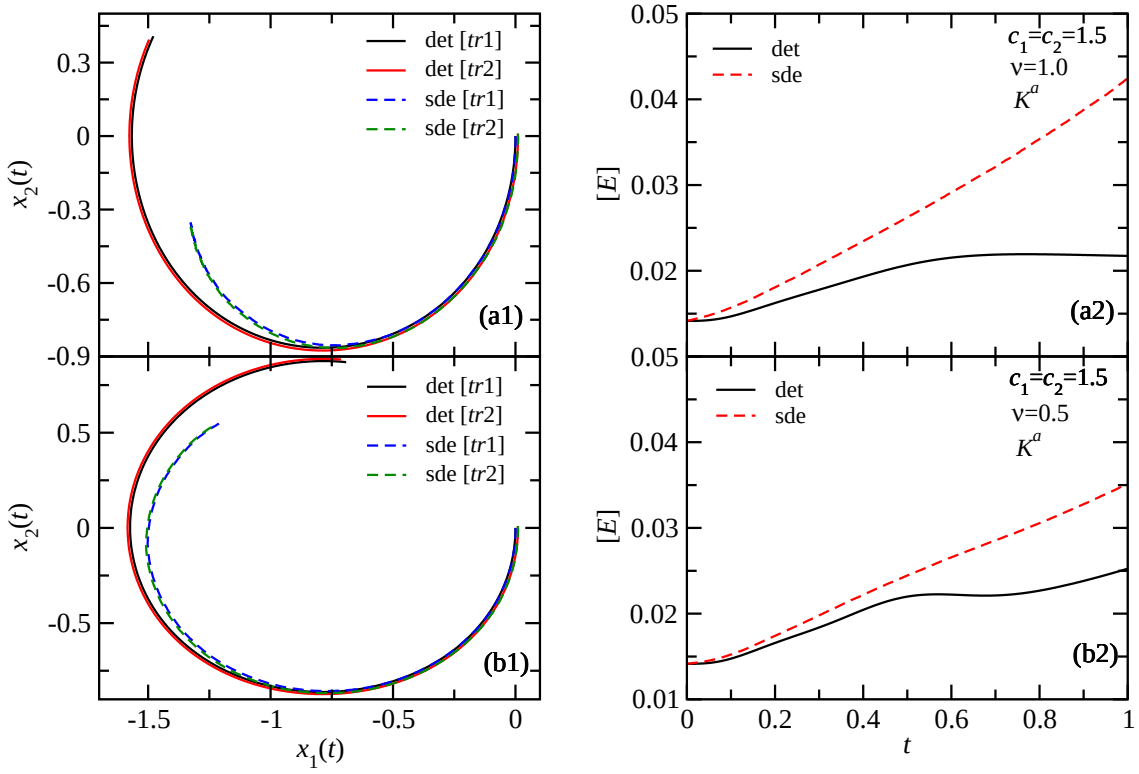

FIGURE 3. Deterministic and stochastic trajectories (a1) and (b1) calculated over the interval $[0, 1]$, along with the distance and, respectively, the expected values of the distance of the stochastic trajectories (a2) and (b2). The trajectories $tr1$ and $tr2$ start respectively, at $(0.0, 0.0)$ and $(0.01, 0.01)$.

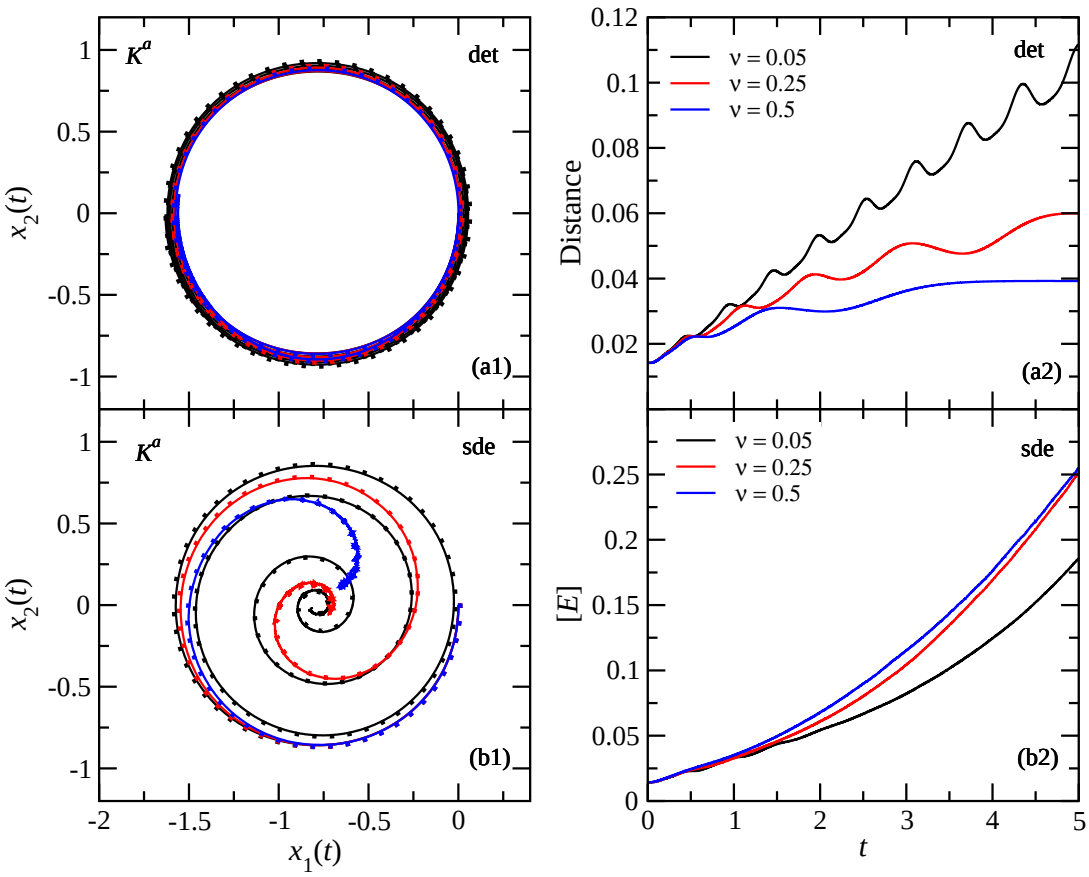

FIGURE 4. Deterministic (a1) and stochastic (b1) trajectories calculated over the interval $[0, 5]$, along with the distance (a2) and, respectively, the expected values of the distance of the stochastic trajectories (b2), for different values of ν. The sums over k for the deterministic and stochastic terms are for K^a. The trajectories, lines and dots, start, respectively, at $(0.0, 0.0)$ and $(0.01, 0.01)$.

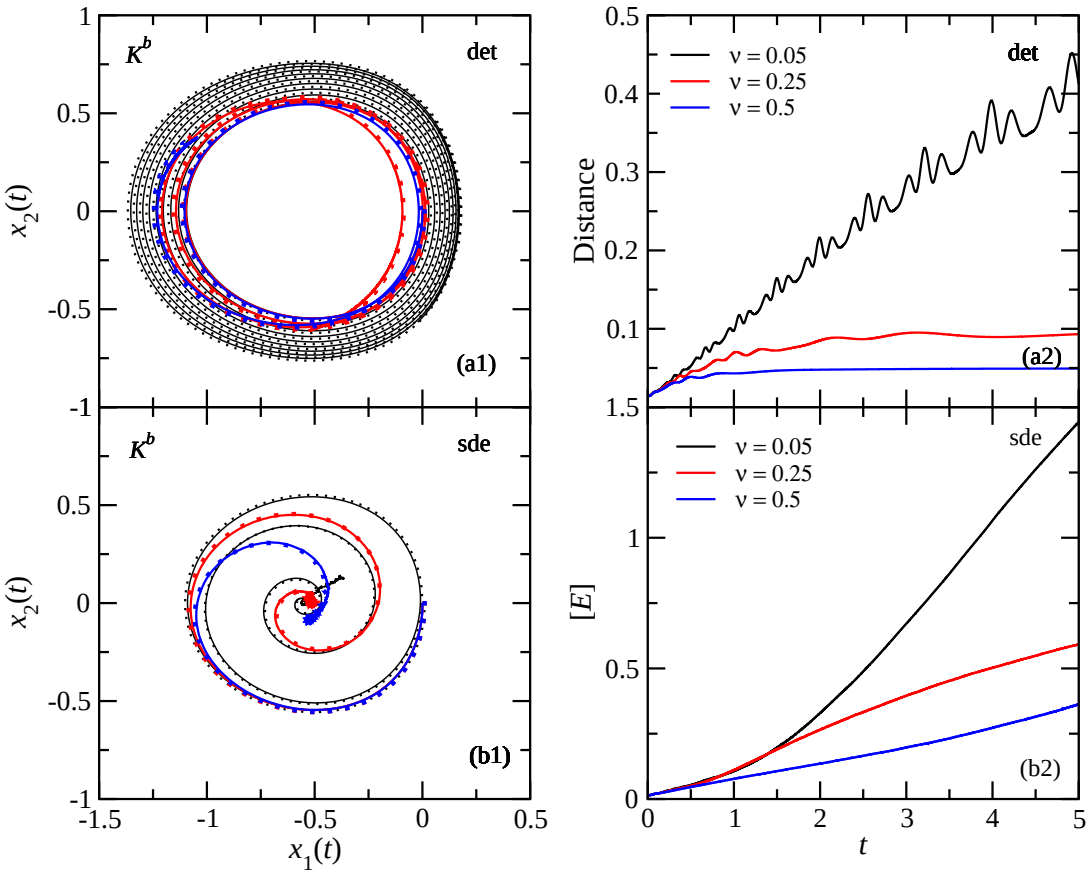

FIGURE 5. Deterministic (a1) and stochastic (b1) trajectories calculated over the interval $[0, 5]$, along with the distance (a2) and, respectively, the expected values of the distance of the stochastic trajectories (b2), for different values of ν. The sums over k for the deterministic term are for K^b and those for the stochastic term are for K^a. The trajectories, lines and dots, start, respectively, at $(0.0, 0.0)$ and $(0.01, 0.01)$.

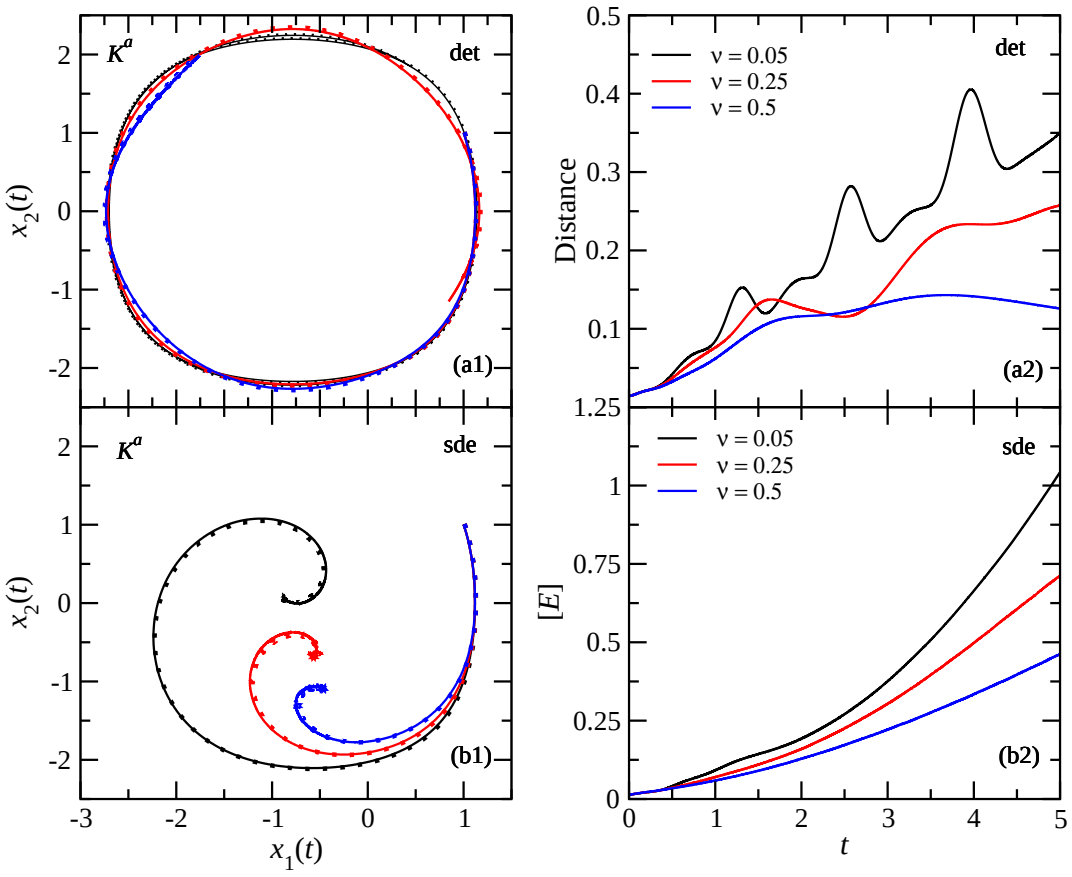

FIGURE 6. Deterministic (a1) and stochastic (b1) trajectories calculated over the interval $[0, 5]$, along with the distance (a2) and, respectively, the expected values of the distance of the stochastic trajectories (b2), for different values of ν. The sums over k for the deterministic and stochastic terms are for K^a. The trajectories, lines and dots, start, respectively, at $(1.0, 1.0)$ and $(1.01, 1.01)$.

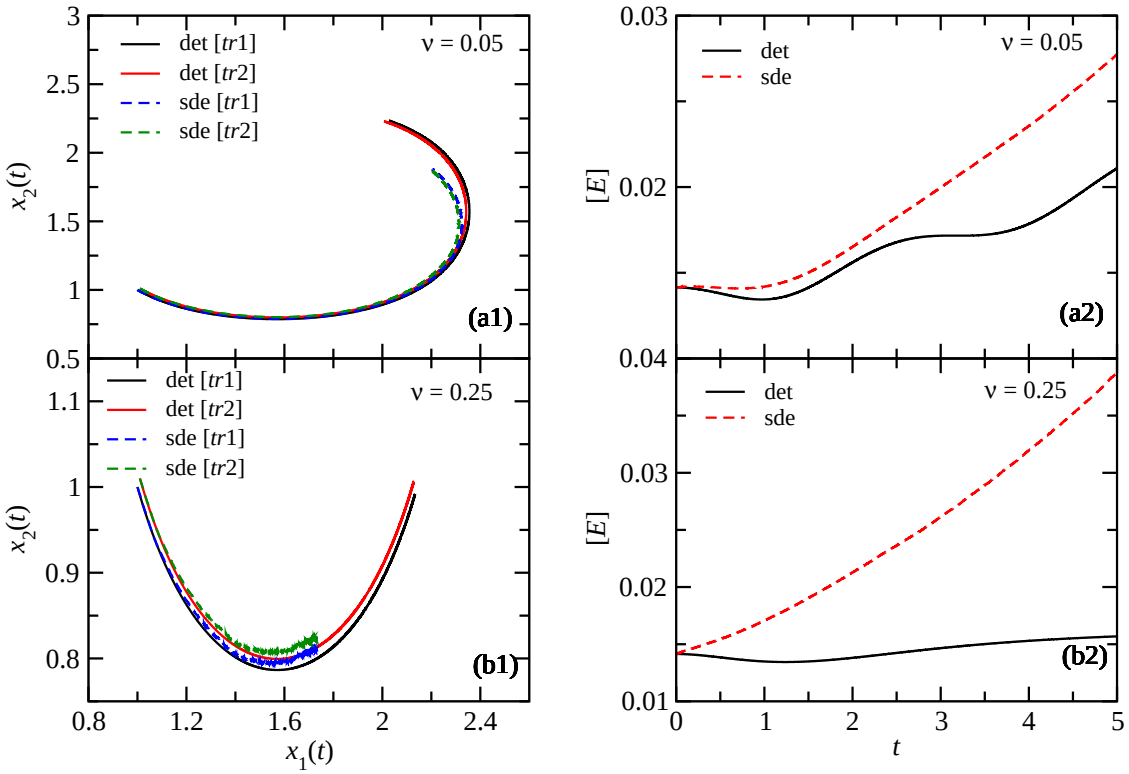

FIGURE 7. Deterministic and stochastic trajectories (a1) and (b1) calculated over the interval $[0, 5]$, along with the distance, and, respectively, the expected values of the distance of the stochastic trajectories (a2) and (b2). The trajectories $tr1$ and $tr2$ start respectively, at $(1.0, 1.0)$ and $(1.01, 1.01)$.

REFERENCES

[1] H. Aref *Stirring by chaotic advection*, J. Fluid Mech., 143, 1984.

[2] M. Arnaudon and A. B. Cruzeiro, *Lagrangian Navier-Stokes diffusions on manifolds: variational principle and stability*, preprint, arXiv:1004.2176.

[3] V. I. Arnold, *Sur la géométrie différentielle des groupes de Lie de dimension infinie et ses applications à l'hydrodynamique des fluides parfaits*, Ann. Inst. Fourier 16 (1966), 316–361.

[4] V. I. Arnold and B. A. Khesin, *Topological methods in hydrodynamics*, Applied Mathematical Sciences, 125, Springer-Verlag, Berlin, 1998.

[5] D. Bernard, K. Gawedzki and A. Kupiainen, *Slow modes in passive advection*, J. Stat. Phys., 90, 34 (1998) 519–569.

[6] Th. Bohr, M. H. Jensen, G. Paladin, and A. Vulpiani, *Dynamical Systems Approach to Turbulence*, Cambridge Nonlinear Sc. Series, 8, 1998.

[7] J. H. Cartwright, M. Feingold and O. Piro, *An introduction to chaotic advection, in Mixing, Chaos and Turbulence*, Eds H. Chaté, E. Villermaux, J. M. Chomez (1999) 307–342.

[8] W. E. and E. Vanden-Eijnden, *Generalized flows, intrinsic stochasticity and turbulent transport*, Proc. Natl. Acad. Sci. USA 97 (2000) 8200–8205.

[9] G. L. Eyink, *Stochastic least-action principle for the incompressible Navier-Stokes equation*, Physica D 239 (2010) 1236–1240.

[10] F. Cipriano and A.B. Cruzeiro, *Navier-Stokes equation and diffusions on the group of homeomorphisms of the torus*, Comm. Math. Phys. 275 (2007), no. 1, 255–269.

[11] P. Constantin and G. Iyer, *A stochastic Lagrangian representation of the three dimensional incompressible Navier-Stokes equations*, Comm. Pure Appl. Math, 61 (2008) no. 3, 330–345.
[12] P. E. Kloeden and E. Platen, *Numerical solutions of stochastic differential equations*, Springer-Verlag, Berlin, 1996.
[13] Y. Le Jan and O. Raimond, *Integration of Brownian vector fields*, Ann. Probab. 30 (2002) 826–873.
[14] T. Nakagomi, K. Yasue and J.-C. Zambrini, *Stochastic variational derivations of the Navier-Stokes equation.* Lett. Math. Phys.,160 (1981), 337–365.
[15] Y. Watanabe, *Differential geometry on diffeomorphism groups and Lagrangian stability.* Physica D, 225 (2007), 197–203.

Laboratoire de Mathématiques et Applications
CNRS: UMR 6086
Université de Poitiers, Téléport 2 - BP 30179
F–86962 Futuroscope Chasseneuil Cedex, France
E-mail address: marc.arnaudon@math.univ-poitiers.fr

GFMUL and Dep. de Matemática IST(TUL).
Av. Rovisco Pais
1049-001 Lisboa, Portugal
E-mail address: abcruz@math.ist.utl.pt

GFMUL.
Av. Prof. Gama Pinto 2
1649-003 Lisboa, Portugal
E-mail address: ngalamba@cii.fc.ul.pt